ACS OMEGA

Article

Cite This: ACS Omega 2018, 3, 9086−9095

http://pubs.acs.org/journal/acsodf

Thermodynamics of the Binding of Lysozyme to a Dendritic Polyelectrolyte: Electrostatics Versus Hydration

Qidi Ran,[†,‡,§] Xiao Xu,[∥] Joachim Dzubiella,[⊥,‡,§] Rainer Haag,[*,†,§] and Matthias Ballauff[*,‡,§,#]

[†]Institute of Chemistry and Biochemistry, Freie Universität Berlin, Takustr. 3, 14195 Berlin, Germany

[‡]Institute of Soft Matter and Functional Materials, Helmholtz-Zentrum Berlin, Hahn-Meitner-Platz 1, 14109 Berlin, Germany

[§]Multifunctional Biomaterials for Medicine, Helmholtz Virtual Institute, Kantstr. 55, 14513 Teltow-Seehof, Germany

[∥]School of Chemical Engineering, Nanjing University of Science and Technology, 200 Xiao Ling Wei, 210094 Nanjing, P. R. China

[⊥]Physikalisches Institut, Albert-Ludwigs-Universität, Hermann-Herder-Str. 3, 79104 Freiburg, Germany

[#]Institut für Physik, Humboldt-Universität zu Berlin, Newtonstr. 15, 12489 Berlin, Germany

Supporting Information

ABSTRACT: The interaction between dendritic polyglycerol sulfate (dPGS) of the second generation and lysozyme was studied by isothermal titration calorimetry (ITC) at different temperatures and salt concentrations. Analysis by ITC showed that 2−3 lysozyme molecules were bound to each dPGS. The resulting binding constant K_b and the Gibbs free energy ΔG^o decreased markedly with increasing salt concentration but were nearly independent of temperature. The salt dependence of K_b led to the conclusion that ca. 3 counterions bound to dPGS were released upon complex formation. The gain in entropy ΔG_{ci} by this counterion-release scales logarithmically with salt concentration and is the main driving force for binding. The temperature dependence of ΔG^o was analyzed by the nonlinear van't Hoff plot, taking into account a finite heat capacity change $\Delta C_{p,vH}$. This evaluation led to the binding enthalpy ΔH_{vH} and the binding entropy ΔS_{vH}. Both quantities varied strongly with temperature and even changed sign, but they compensated each other throughout the entire range of temperature. Coarse-grained computer simulations with explicit salt and implicit water were used to obtain the binding free energies that agreed with ITC results. Thus, electrostatic factors were the driving forces for binding whereas all hydration contributions leading to the strongly varying ΔH_{vH} and ΔS_{vH} canceled out. The calorimetric enthalpy ΔH_{ITC} measured directly by ITC differed largely from ΔH_{vH}. ITC measurements done in two buffer systems with different ionization enthalpies revealed that binding was linked to buffer ionization and a partial protonation of the protein.

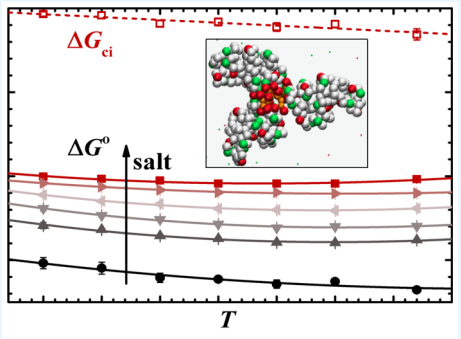

INTRODUCTION

The interaction of proteins with polyelectrolytes is a long-standing subject in biochemistry, drug design, and materials science.[1−5] Many biopolymers, for example DNA, are highly charged and interact with proteins via electrostatic forces.[6] Proteins may form complexes with natural or synthetic polyelectrolytes of opposite charge ("complex coacervates" cf. refs 2 and 3) that have applications as food colloids.[5] Central to this field is the investigation of the equilibrium binding constant between a given protein and a polyelectrolyte in order to explore the various thermodynamic factors that lead to binding. Isothermal titration calorimetry (ITC) has become a pivotal technique to explore the thermodynamics of ligands binding with proteins.[7−9] The heat signal measured directly by ITC can be converted to the binding constant K_b, the temperature dependence of which may then yield the enthalpy and entropy of binding ΔH_b and ΔS_b, respectively.[10−12] The total heat ΔH_{ITC} also furnished by ITC need not agree with ΔH_b because linked equilibria may also contribute to the heat signal.[13,14] It is thus evident that ITC can be used to explore the full thermodynamics of binding between polyelectrolytes and proteins. However, the use of these data for the design of drugs may be difficult and in parts questionable.[15] Additional information furnished by computer simulations using coarse-grained (CG) and molecular models would clearly be helpful to clarify the details of binding in order to use these data for drug design and for predicting the binding constants of polyelectrolytes to a given protein.

We have recently shown that ITC data can directly be combined with molecular dynamics (MD) simulations.[16] As a model polyelectrolyte, we used the dendritic polyglycerol sulfate (dPGS). The scaffold of these dPGS dendrimers is made up from a hyperbranched polyglycerol core. Sulfate groups attached to all terminals render these molecules very hydrophilic and highly charged. dPGS has been shown to be promising drug and carrier recently.[17−23] It has also been the

Received: June 29, 2018
Accepted: July 30, 2018
Published: August 14, 2018

DOI: 10.1021/acsomega.8b01493
ACS Omega 2018, 3, 9086−9095

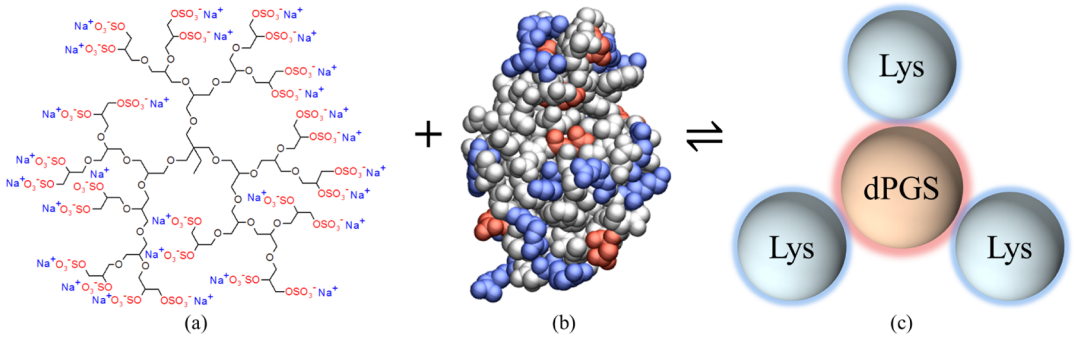

Figure 1. (a) Chemical representative of the dPGS. (b) Molecular structure of lysozyme (PDB: 2LZT).[26] The blue, red, and white beads represent positive, negative, and neutral amino acids, respectively. (c) Idealized sketch of the dPGS–Lys complex taking all molecules as spheres. The overall positive lysozymes and negative dPGS are characterized with blue and red surfaces, respectively. The stoichiometry of complexation is ~3 at 310 K and 10 mM salt purely driven by electrostatic interaction.[16]

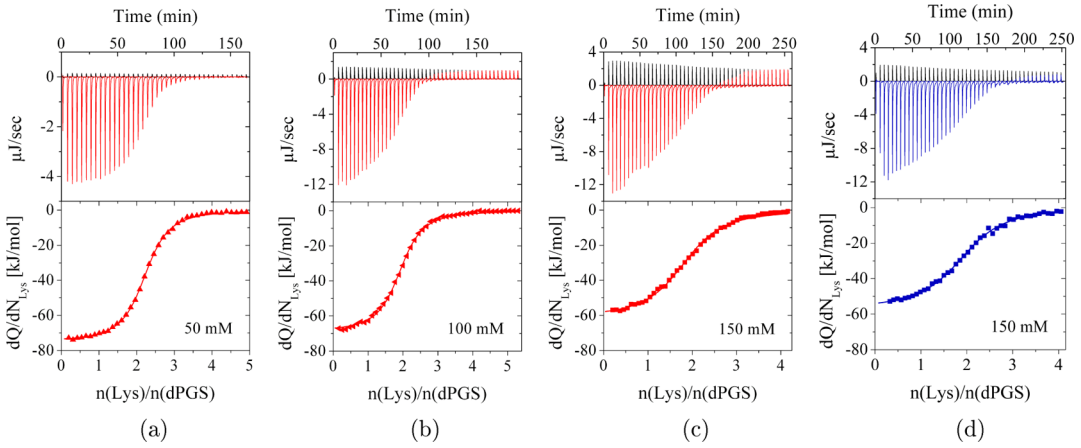

Figure 2. ITC isotherms in phosphate buffer pH 7.4 at ionic strengths: (a) 50, (b) 100, and (c) 150 mM at 310 K. (d) Isotherm in MOPS buffer at 150 mM and 310 K done in ref 16. The black peaks in the upper panels represent the dilution heat of lysozyme into respective buffer which will be subtracted from the adsorption heat. The signal gets stronger at higher ionic strength because of higher sample concentration. The red and blue peaks are the adsorption heat into dPGS solutions. The symbols in the lower panel are the integrated molar heat for each titration related to the added protein. The solid curves are fitted by the SSIS model.

subject of a comprehensive study by computer simulation[24] and can be considered a well-controlled model polyelectrolyte. Figure 1 displays the chemical structure of a dPGS. The synthesized dPGS with a hyperbranched structure[25] comes close to the perfect dPGS dendrimer of generation 2 (see the discussion in ref 24).

In our recent study, ITC and computer simulations with implicit water were used to study the binding of lysozyme to dPGS of different generations.[16] This investigation demonstrated that the interaction of the dPGS dendrimers with proteins can be traced back mainly to electrostatic effects. The main part of the electrostatic interaction was shown to be counterion-release: a part of the counterions condensed to the polyelectrolyte dPGS[24] is released upon binding of the protein. Counterion condensation and release influence the thermodynamics of a polyelectrolyte and its complex formation with other molecules.[27] The released counterions increase the entropy of the system. The decrease of Gibbs free energy ΔG° scales therefore with ln c_s, where c_s denotes the salt concentration in the solution.[6,28] In addition to this, the screened electrostatic attraction on the Debye–Hückel (DH) level between the negatively charged dPGS and the positively charged lysozyme plays a role at low concentration of added salt.[16] We found that the binding constant derived from MD-simulations with explicit ions but implicit water fully agreed with the experimental values derived by ITC. The same result was obtained in a recent study of the binding of poly(acrylic acid) to human serum albumin (HSA) by both ITC and computer simulations.[29] These findings led to the conclusion that electrostatic terms dominate the binding of charged polymers to proteins to a large extend.

To elucidate this point further, we have recently performed a comprehensive thermodynamic investigation of the binding of HSA to dPGS by ITC.[30] The binding constant K_b was measured at different temperatures at low salt concentration. In addition to this, the dependence of the binding constant on salt concentration was determined. Then, the analysis on the binding constant K_b of the 1:1 complex of HSA and dPGS-G2 demonstrated that the binding free energy depended hardly on temperature. However, both the binding enthalpy and entropy were found to vary strongly with temperature but compensated each other. This enthalpy–entropy compensation (EEC) has been observed in many systems by now[15,31−35] and is related to a high value of the heat capacity change ΔC_p. It is clearly seen also in systems of biological relevance.[10−12]

Here, we extend these investigations to the binding of dPGS-G2 to lysozyme using again a systematic variation of both the salt concentration and the temperature. In this way, the electrostatic factors contributing to binding can be separated from hydrophilic/hydrophobic hydration/dehydra-

DOI: 10.1021/acsomega.8b01493
ACS Omega 2018, 3, 9086−9095

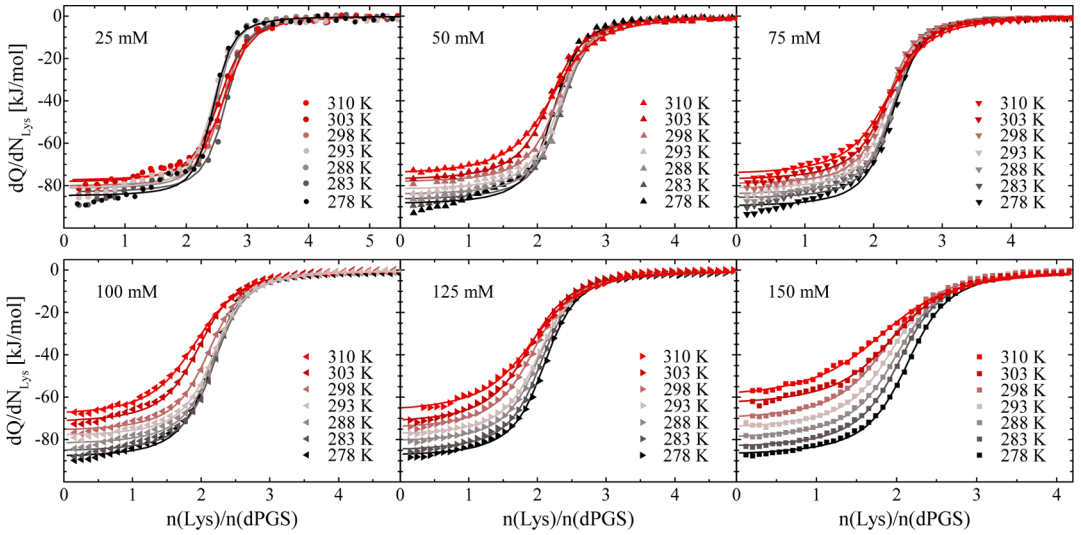

Figure 3. ITC isotherms for dPGS-G2 binding with lysozyme in phosphate buffer pH 7.4 with ionic strengths: 25, 50, 75, 100, 125, and 150 mM at different temperatures. The solid lines present the fits by the SSIS model.

tion. The EEC can hence be studied in detail for this system, which will allow us to discuss the role of thermodynamic quantities for predicting the interaction of proteins with highly charged macromolecules. In addition to these experimental studies, we extend our previous MD simulations of the system dPGS/lysozyme.[16] Special effort is laid to the direct comparison of the data obtained by experiments and simulations. In this context, it is revealing to consider the various contributions to the enthalpy ΔH_{ITC} measured directly by ITC. The entire set of data will allow us a comprehensive discussion of the use of thermodynamic data when discussing and predicting thermodynamic equilibria between proteins and highly charged macromolecules.

RESULTS AND DISCUSSION

The complex formation of lysozyme with dPGS of different generations was studied recently by ITC and computer simulations at 310 K and 10 mM salt concentration.[16] Lysozyme has a net charge of +8 *e* at physiological pH. The synthetic dPGS-G2 bears −28 *e* total charges while its effective charge is −11 *e* in solution because of counterion condensation.[24] Figure 1 sketches the adsorption process for dPGS-G2. We found that approximately 3 lysozyme molecules and 1 dPGS form a complex with $K_b \approx 10^8$ M^{-1} at 10 mM salt.[16] The sulfate terminal groups bind with positive patch on the protein, thereby releasing ca. 3 counterions bound to dPGS. In the present work, all binding experiments are done in phosphate buffer whereas the experiments in ref 16 were done in 3-(*N*-morpholino)propanesulfonic acid (MOPS) buffer. Here, we chose the phosphate buffer because the adjusted pH hardly changes with temperature.[36] In addition, the use of different buffers will allow us to discern possible heat contributions from the buffer aside from binding.[13,14]

The raw data of the titration peaks and the respective isotherms at 310 K and c_s = 50, 100, 150 mM are shown in Figure 2. The interaction is exothermic under all conditions. All the parameters including binding number *N*, binding constant K_b, and ITC enthalpy ΔH_{ITC} could be obtained very well by fitting the data with the single set of identical sites (SSIS) model.[37] Figure 3 gives a survey of all ITC isotherms together with the respective fits referring to all salt concentrations and temperatures under consideration here. Table 1 summarizes all fit parameters obtained from ITC experiments. The number *N* of bound lysozyme molecules decreases slightly with salt concentration but stays approximately constant with temperature. In the present salt concentration of 25 mM, it is found slightly smaller than previously observed 3−4 in 10 mM MOPS buffer.[16] The binding affinity of lysozyme with dPGS decreases with salt concentration as expected. Table 1 furthermore shows that the binding free energy ΔG^o hardly changes with temperature but decreases significantly with increasing ionic strength.

Electrostatic and Steric Contributions to the Binding Affinity. The electrostatic interaction between oppositely charged polyelectrolytes has been used for many decades in areas such as multilayer film formation.[38,39] In our previous study, we discussed the electrostatic contributions to the binding between dPGS and lysozyme. On the basis of a comparison of ITC data with MD simulations, we found that the binding was mainly driven by counterion-release.[16] Simulations of the highly charged dPGS dendrimers[24] demonstrated that there was a thin shell or Stern layer of condensed counterions on the surface of the dendrimers. From this, a surface concentration of condensed counterions c_{ci} can be estimated (see Table S3 of ref 16). In the case of G2, c_{ci} = 0.96 M is much higher than the salt concentrations in bulk used here in the ITC-runs. When lysozyme is bound to dPGS, the positive patch on the surface of the protein becomes a multivalent counterion to the dendrimer. A concomitant number of the condensed counterions of dPGS are thereby released into the bulk solution. The corresponding gain of entropy follows as

$$\Delta G_{ci} = -T\Delta S_{ci} = -\Delta N_{ci} k_B T \ln(c_{ci}/c_s) \quad (1)$$

where c_{ci} and c_s are the concentrations of local condensed counterions and bulk salt, respectively, and ΔN_{ci} is the number of released counterions.[16,40] From this, it follows that the binding constant is related to ΔN_{ci} if counterion-release is a dominant driving force[6,28]

$$\frac{d\ln K_b}{d\ln c_s} = -\Delta N_{ci} \quad (2)$$

DOI: 10.1021/acsomega.8b01493
ACS Omega 2018, 3, 9086−9095

Table 1. Thermodynamic Properties of Lysozyme Binding to dPGS-G2 in Phosphate Buffer pH 7.4 under Different Conditions[a]

c_s [mM]	T [K]	N	K_b [10^5 M^{-1}]	ΔG° [kJ/mol] (k_BT)	ΔH_{ITC} [kJ/mol]	ΔH_{vH} [kJ/mol]	$T\Delta S_{vH}$ [kJ/mol]	$\Delta C_{p,ITC}$ [kJ/(mol K)]	$\Delta C_{p,vH}$ [kJ/(mol K)]
25	278	2.4 ± 0.02	384 ± 99	−40.4 ± 0.7(−17.5)	−84.9 ± 0.8	3.5 ± 12.3	43.9 ± 12.0	0.22 ± 0.02	−1.20 ± 0.75
	283	2.6 ± 0.03	362 ± 110	−41.0 ± 0.7(−17.4)	−83.1 ± 0.9	−2.5 ± 8.7	38.6 ± 8.7		
	288	2.4 ± 0.02	433 ± 100	−42.1 ± 0.6(−17.6)	−81.3 ± 0.7	−8.5 ± 5.5	33.3 ± 5.6		
	293	2.4 ± 0.01	345 ± 48	−42.3 ± 0.3(−17.4)	−81.3 ± 0.7	−14.4 ± 3.6	27.8 ± 3.6		
	298	2.5 ± 0.02	325 ± 65	−42.9 ± 0.5(−17.3)	−80.4 ± 0.6	−20.4 ± 4.9	22.3 ± 4.9		
	303	2.5 ± 0.01	216 ± 20	−42.5 ± 0.3(−16.9)	−78.6 ± 0.5	−26.4 ± 8.0	16.6 ± 8.0		
	310	2.5 ± 0.01	217 ± 20	−43.5 ± 0.2(−16.9)	−77.7 ± 0.5	−34.8 ± 12.9	8.6 ± 13.1		
50	278	2.2 ± 0.02	55.1 ± 9.3	−35.9 ± 0.4(−15.5)	−88.9 ± 0.7	11.7 ± 4.8	47.4 ± 4.7	0.43 ± 0.03	−1.99 ± 0.29
	283	2.3 ± 0.01	51.7 ± 3.9	−36.4 ± 0.2(−15.5)	−86.8 ± 0.5	1.7 ± 3.4	38.2 ± 3.4		
	288	2.3 ± 0.01	53.7 ± 4.1	−37.1 ± 0.2(−15.5)	−84.4 ± 0.5	−8.3 ± 2.2	28.8 ± 2.2		
	293	2.3 ± 0.01	47.5 ± 3.7	−37.5 ± 0.2(−15.4)	−82.1 ± 0.5	−18.2 ± 1.4	19.3 ± 1.4		
	298	2.3 ± 0.01	43.8 ± 1.9	−37.9 ± 0.1(−15.3)	−78.6 ± 0.3	−28.2 ± 1.9	9.6 ± 1.9		
	303	2.2 ± 0.01	34.7 ± 1.7	−37.9 ± 0.1(−15.1)	−77.5 ± 0.4	−38.2 ± 3.1	−0.3 ± 3.1		
	310	2.2 ± 0.01	21.7 ± 1.1	−37.6 ± 0.1(−14.6)	−74.9 ± 0.2	−52.2 ± 5.0	−14.4 ± 5.1		
75	278	2.3 ± 0.02	22.8 ± 3.1	−33.8 ± 0.3(−14.6)	−90.1 ± 0.5	16.4 ± 3.8	50.2 ± 3.8	0.46 ± 0.02	−2.06 ± 0.24
	283	2.2 ± 0.01	25.2 ± 2.2	−34.7 ± 0.2(−14.7)	−86.2 ± 0.6	6.1 ± 2.7	40.7 ± 2.7		
	288	2.2 ± 0.01	23.9 ± 1.9	−35.2 ± 0.2(−14.7)	−84.3 ± 0.5	−4.2 ± 1.7	31.1 ± 1.7		
	293	2.2 ± 0.01	23.3 ± 1.7	−35.7 ± 0.2(−14.7)	−81.7 ± 0.5	−14.5 ± 1.1	21.2 ± 1.1		
	298	2.2 ± 0.01	21.7 ± 1.5	−36.1 ± 0.2(−14.6)	−79.5 ± 0.4	−24.8 ± 1.5	11.2 ± 1.5		
	303	2.2 ± 0.01	16.1 ± 0.9	−36.0 ± 0.1(−14.3)	−77.6 ± 0.4	−35.1 ± 2.5	1.0 ± 2.5		
	310	2.2 ± 0.01	11.5 ± 0.6	−36.0 ± 0.1(−14.0)	−75.1 ± 0.4	−49.5 ± 4.0	−13.6 ± 4.1		
100	278	2.1 ± 0.01	11.4 ± 1.0	−32.2 ± 0.2(−13.9)	−88.5 ± 0.4	11.0 ± 3.0	43.2 ± 3.0	0.63 ± 0.02	−1.89 ± 0.19
	283	2.2 ± 0.01	12.2 ± 0.7	−33.0 ± 0.1(−14.0)	−85.8 ± 0.4	1.6 ± 2.2	34.5 ± 2.1		
	288	2.2 ± 0.01	11.0 ± 0.6	−33.3 ± 0.1(−13.9)	−82.4 ± 0.4	−7.9 ± 1.4	25.6 ± 1.4		
	293	2.2 ± 0.01	10.9 ± 0.5	−33.9 ± 0.1(−13.9)	−78.6 ± 0.4	−17.3 ± 0.9	16.5 ± 0.9		
	298	2.1 ± 0.01	9.2 ± 0.4	−34.0 ± 0.1(−13.7)	−76.3 ± 0.3	−26.7 ± 1.2	7.3 ± 1.2		
	303	2.0 ± 0.01	7.6 ± 0.4	−34.1 ± 0.1(−13.5)	−72.2 ± 0.4	−36.2 ± 2.0	−2.1 ± 2.0		
	310	1.9 ± 0.01	5.0 ± 0.2	−33.8 ± 0.1(−13.1)	−69.1 ± 0.4	−49.4 ± 3.2	−15.5 ± 3.2		
125	278	2.1 ± 0.01	6.2 ± 0.4	−30.8 ± 0.2(−13.3)	−88.0 ± 0.3	−3.4 ± 2.0	27.4 ± 1.9	0.65 ± 0.02	−1.11 ± 0.12
	283	2.1 ± 0.01	5.9 ± 0.2	−31.3 ± 0.1(−13.3)	−85.6 ± 0.2	−9.0 ± 1.4	22.3 ± 1.4		
	288	2.0 ± 0.01	5.5 ± 0.1	−31.6 ± 0.1(−13.2)	−81.4 ± 0.2	−14.6 ± 0.9	17.1 ± 0.9		
	293	2.0 ± 0.01	4.9 ± 0.1	−31.9 ± 0.1(−13.1)	−78.3 ± 0.2	−20.1 ± 0.6	11.7 ± 0.6		
	298	2.0 ± 0.01	4.0 ± 0.2	−31.9 ± 0.1(−12.9)	−75.2 ± 0.3	−26.7 ± 0.8	6.3 ± 0.8		
	303	1.9 ± 0.01	3.4 ± 0.2	−32.1 ± 0.1(−12.7)	−72.5 ± 0.4	−31.3 ± 1.3	0.8 ± 1.3		
	310	2.0 ± 0.02	2.5 ± 0.3	−32.0 ± 0.3(−12.4)	−67.2 ± 0.6	−39.1 ± 2.1	−7.0 ± 2.1		
150	278	2.1 ± 0.01	4.4 ± 0.02	−30.1 ± 0.1(−13.0)	−87.6 ± 0.2	−3.2 ± 4.3	26.8 ± 4.2	0.88 ± 0.04	−1.47 ± 0.27
	283	2.1 ± 0.01	4.0 ± 0.09	−30.3 ± 0.1(−12.9)	−84.2 ± 0.2	−10.5 ± 3.1	19.8 ± 3.1		
	288	2.0 ± 0.01	3.4 ± 0.08	−30.5 ± 0.1(−12.7)	−79.9 ± 0.2	−17.9 ± 1.9	12.8 ± 2.0		
	293	2.0 ± 0.01	3.2 ± 0.1	−30.9 ± 0.1(−12.7)	−75.2 ± 0.3	−25.2 ± 1.3	5.6 ± 1.3		
	298	1.9 ± 0.01	2.6 ± 0.1	−30.9 ± 0.1(−12.5)	−71.0 ± 0.4	−32.3 ± 1.7	−1.7 ± 1.7		
	303	2.0 ± 0.01	2.1 ± 0.1	−30.9 ± 0.1(−12.3)	−64.0 ± 0.4	−39.9 ± 2.8	−9.1 ± 2.8		
	310	1.9 ± 0.01	1.3 ± 0.07	−30.4 ± 0.1(−11.8)	−60.9 ± 0.5	−50.2 ± 4.5	−19.9 ± 4.6		

[a] N, K_b, and ΔH_{ITC} are fitting parameters by ITC. ΔG° is calculated according to eq 6. $\Delta C_{p,ITC}$ is the linear dependence of ΔH_{ITC} on temperature obtained from Figure 8. ΔH_{vH}, ΔS_{vH}, and $\Delta C_{p,vH}$ are the binding enthalpy, entropy, and heat capacity change fitted by eq 6, respectively.

Figure 4 presents the dependence of the binding constant on salt concentration. The number of released counterions ranges between 2.5 and 2.7 (data referring to other temperatures are shown in the Supporting Information), which is in accord with our previous result where ΔN_{ci} = 3.1 in MOPS buffer at 310 K.[16] The released counterions from the dPGS surface upon binding can also be monitored by computer simulations,[16] and the results agree with experiments (see Supporting Information). Because c_{ci} equals to 0.96 M at 310 K for dPGS-G2,[24] eq 1 predicts ΔG_{ci} at 25 mM salt concentration to be −9.8 k_BT. It hence presents a major contribution in the total binding free energy. The solid lines in Figure 4 referring to different temperatures are approximately parallel so the number of released counterions does not depend on temperature within the limits of error. It thus demonstrates that counterion-release does not contribute to the heat capacity ΔC_p on this level of approximation.

In addition to counterion-release, there is a DH attraction ΔG_{ele} between dPGS and the bound lysozyme. Moreover, there is an electrostatic repulsion between bound proteins. Considering all the charged beads individually, the pairwise charge−charge interaction on the DH level was summarized by computer simulation.[16] The resultant overall electrostatic interaction between lysozyme and dPGS-G2 was attractive and decreased slightly with the uptake of bound proteins. For the first three bound proteins at c_s = 10 mM, the attraction was

DOI: 10.1021/acsomega.8b01493
ACS Omega 2018, 3, 9086−9095

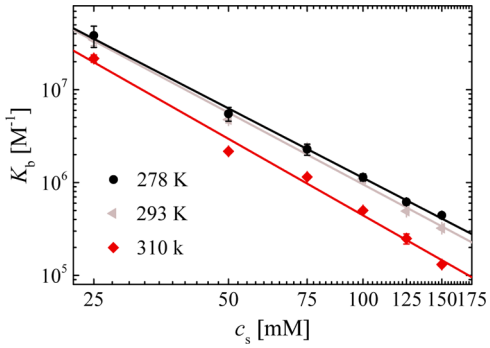

Figure 4. Dependence of binding constant on salt concentration for three different temperatures. The number of released counterions ΔN_{ci} from the slope of these lines fitted according to eq 2 is 2.5 ± 0.1 at 278 K, 2.6 ± 0.1 at 293 K, and 2.7 ± 0.1 at 310 K in phosphate buffer. ΔN_{ci} measured in MOPS buffer at 310 K is 3.1 ± 0.1.[16]

found similar to be −26 kJ/mol (−10 k_BT) (see Figure 2D in ref 16).

Steric repulsion between the bound lysozymes enters as a third term. This packing penalty is non-existent for the first uptake and positive for the subsequent proteins. It becomes a limiting factor when the packing of the proteins leads to a more or less full coverage of the surface. For the situation encountered for G2 where 4 lysozymes are bound, simulations showed this term to be of minor importance.[16]

The findings above lead to the conclusion that the binding free energy of subsequent lysozymes is not a constant but decreases with the number of bound proteins. The Langmuir model which is the basis of the SSIS fitting, on the other hand, assumes that each bound protein is attached independently and the free energy of binding is equivalent for all bound proteins.

To elucidate the cooperativity in a multivalent binding, we measured the complexation of lysozyme with dPGS-G2 for different coordination numbers i by MD simulations. Figure 5

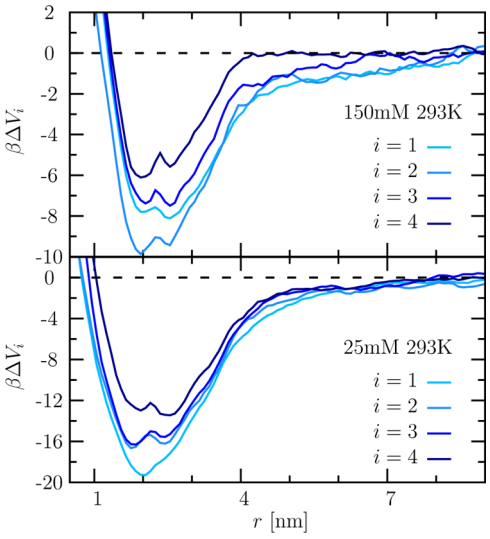

Figure 5. PMF curves $\beta\Delta V_i$ for the complexation between dPGS-G2 and lysozyme vs the dPGS−lysozyme center of mass distance r. ΔV_i is in the unit of k_BT ($\beta = 1/k_BT$). The binding coordination number i ranges from 1 to 4 as indicated in the graph. The simulation was done at T = 293 K and salt concentration c_s = 25 mM (lower panel) and 150 mM (upper panel).

shows the potential of mean force (PMF) profile at 293 K and two salt concentrations. The respective local minimum reveals the binding distance r_b and binding free energy ΔG_b^{sim} at the given coordination number. The complexation between dPGS and the first bound lysozyme is purely driven by electrostatic effects with a binding free energy −27 k_BT at 10 mM salt (see the discussion of Figure 2C in ref 16). The magnitude of ΔG_b^{sim} decreases with i, which indicates a negative cooperativity caused by electrostatic repulsion and steric hindrance.

To account for this negative cooperativity, we recently developed a new way of comparing ΔG_b between the simulation and ITC experiments:[16] in canonical simulations, the concentration c_{bound} of bound and non-interacting ligands follows as[16]

$$c_{bound} = \frac{i}{V_b} = c_{free} \exp(-\beta \Delta G_b) \tag{3}$$

where c_{free} is the concentration of free (unbound) ligands and V_b refers to the effective volume in which the bound ligands are confined. ΔG_b defines the transfer free energy from bulk to the bound state, which can be taken directly from the minimum of the PMF profile.[16] We now assume that the binding complex consists of i lysozyme ligands bound in a shell on the surface of dPGS which are idealized as spheres. Hence, the binding volume $V_b = 4\pi(r_b)^2\delta_b$. We take the binding distance r_b = 2.5 nm at saturation together with the thickness of the spherical binding shell δ_b = 1 nm.

In the Langmuir model used for the evaluation of the experiments, the protein coverage θ is defined as

$$\theta = \frac{i}{N} = c_{free} K_b (1 - \theta) \tag{4}$$

with $K_b = v_0 \exp(-\beta \Delta G^\circ)$ the binding constant related to the Langmuir binding free energy ΔG° in Table 1. Here, the volume prefactor v_0 is defined to be 1 L/mol. Combination of eq 3 with 4 leads to the "simulation-referenced" Langmuir *free energy* by

$$\Delta G_b^{ITC} = \Delta G^\circ - k_BT \ln(1 - \theta^*) - k_BT \ln(v_0 N / V_b) \tag{5}$$

which leads to a direct comparison between the experimental ITC curves and the simulations discussed previously.[16] The degree of coverage θ^* is obtained from the inflection point of the ITC isotherms, where $n(\text{Lys})/n(\text{dPGS}) = N$ and is smaller than unity.[16]

We apply this method to the present data and find θ^* at four different conditions (see Supporting Information). ΔG_b^{ITC} at the inflection point can then be calculated with eq 5 and compared to ΔG_b^{sim} in Figure 6. We find a full agreement between simulation and ITC for all conditions. Thus, the experimental results can be rationalized very well in terms of the simulations.

It is interesting to note that the data taken at higher salt concentration exhibit a much weaker dependence on θ (squares in Figure 6) than the ones obtained for lower salt concentrations (circles). This means that the binding affinity at c_s = 150 mM shows much lower negative cooperativity, which can be traced back to the weaker DH interaction in the presence of more salt. At the same time, the simulations confirm a weak dependence of ΔG_b on temperature consistent with the experimental data.

A meaningful comparison of ΔG° measured at different conditions requires that θ^* remains constant under all

DOI: 10.1021/acsomega.8b01493
ACS Omega 2018, 3, 9086−9095

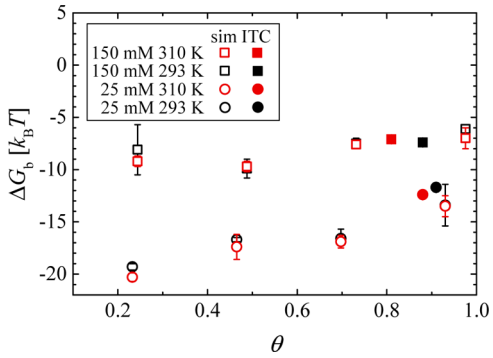

Figure 6. Binding free energy ΔG_b^{sim} vs the protein coverage $\theta = i/N^{sim}$, where i is the binding coordination number and N^{sim} is the binding stoichiometry from simulations. ΔG_b^{sim} values by simulations at different conditions are depicted by the empty symbols. These results are compared with the "simulation-referenced" Langmuir *free energy* ΔG_b^{ITC} according to eq 5 at θ^*, denoted by the filled points.

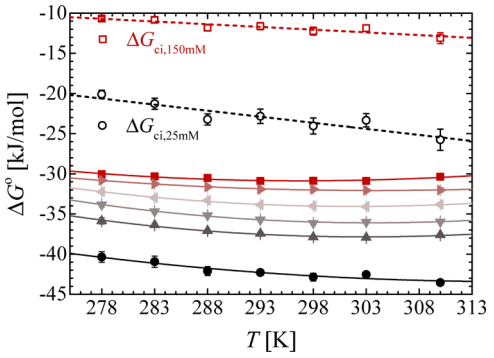

Figure 7. Nonlinear van't Hoff analysis for dPGS−Lys complexation at different ionic strengths according to eq 6: 25 mM (●), 50 mM (▲), 75 mM (▼), 100 mM (◀), 125 mM (▶), and 150 mM (■). The counterion-release entropy gain ΔG_{ci} is calculated with ΔN_{ci} according to eq 1.

conditions. Table 1 shows that the number N of bound lysozymes measured for a given salt concentration does not depend on temperature. Therefore, the present set of data can be used to discuss the dependence on temperature without restrictions. There are small changes of N for a given temperature when going from low salt concentrations to higher ones. However, this change can be disregarded in good approximation. Hence, the data gathered in Table 1 allow us to discuss the dependence of ΔG^o on both salt concentration and temperature which is done in the following.

Enthalpy−Entropy Compensation. As discussed above, the accuracy of the obtained ΔG^o is fully sufficient for a meaningful analysis of the dependence on T. Previous work on complex formation of proteins with nucleic acids has clearly revealed that the binding enthalpy depends markedly on temperature,[11,12] which shows that the heat capacity change ΔC_p is of appreciable magnitude. Therefore, the binding free energy must be rendered in terms of the nonlinear van't Hoff relation[11,41]

$$\begin{aligned}\Delta G^o &= -RT \ln K_b \\ &= \Delta H_{vH,ref} - T\Delta S_{vH,ref} \\ &\quad + \Delta C_{p,vH}\left[(T - T_{ref}) - T \ln\left(\frac{T}{T_{ref}}\right)\right]\end{aligned} \tag{6}$$

where $\Delta H_{vH,ref}$ and $\Delta S_{vH,ref}$ are the binding enthalpy and entropy, respectively, at a given reference temperature T_{ref}.

The analysis of the data shown in Figure 7 according to eq 6 is done as follows: the given temperature is chosen as reference temperature T_{ref}, and the corresponding binding enthalpy $\Delta H_{vH,ref}$, entropy $\Delta S_{vH,ref}$, and heat capacity change $\Delta C_{p,vH}$ are obtained as fit parameters. This procedure is done for all temperatures under consideration here. The values ΔH_{vH}, ΔS_{vH}, and $\Delta C_{p,vH}$ obtained for all temperatures by this fit are listed in Table 1. Here, $\Delta C_{p,vH}$ has been treated as a freely floating parameter but the fit results are constant for each salt concentration.

The curvature in Figure 7 which is due to the heat capacity $\Delta C_{p,vH}$ is similar and the data are of sufficient precision to determine this quantity. $\Delta C_{p,vH}$ is constant in this range of temperature and approximately −2 kJ/(mol K) for all the ionic strengths. Both ΔH_{vH} and ΔS_{vH} change strongly with temperature, whereas ΔG^o is nearly a constant. This insensitivity of ΔG^o to T necessarily leads to a marked EEC considering a large $\Delta C_{p,vH}$.

Figure 7 also contains the part ΔG_{ci} calculated for 25 and 150 mM salt by eq 1. The magnitude of ΔG_{ci} varies linearly with temperature, which is obvious from eq 1: $\Delta S_{ci} = \Delta N_{ci} k_B \ln(c_{ci}/c_s)$ does not depend on T if one disregards small change of c_{ci} with temperature. The difference between ΔG_{ci} and ΔG^o is mainly due to the electrostatic interaction ΔG_{ele} as discussed above and in ref 16. At constant temperature, for example 293 K, this electrostatic part can be read off to be −19 kJ/mol at both 25 and 150 mM salt from Figure 7. It does not vanish with added salt as expected for a simple DH-interaction. Thus, the analytical modeling of the electrostatic interaction between the protein adhering directly to the dendritic polyelectrolyte requires a more detailed description containing higher order multipole terms. It should be noted, however, that the simulation carries along all necessary contributions because it fully agrees with the experimental data.

Figure 8 depicts the entropic and enthalpic contributions in the total free energy at all ionic strengths. It demonstrates directly the EEC. ΔH_{vH} and ΔS_{vH} even change sign in most cases in Figure 8, whereas ΔG^o is almost constant. It is thus evident that the EEC is leading to a nearly constant free energy of binding because ΔH_{vH} and $T\Delta S_{vH}$ run strictly parallel within the present window of temperature. Hence, for our system, the enthalpic and entropic changes with temperature due to hydration effects seem to cancel out each other nearly completely. In general, EEC is a commonly observed phenomenon for binding of polyelectrolytes with proteins.[32,33,42] This effect has widely frustrated the use of thermodynamic data for drug design.[15] The present discussion underscores this problem and accentuates that one should strive to calculate binding free energy rather than enthalpic or entropic contributions individually.

Figure 8 shows clearly that ΔH_{vH} deviates markedly from the directly measured ΔH_{ITC}, which is different from the dPGS−HSA binding system in our previous study.[30] It is well-known that ΔH_{ITC} measured directly in the calorimetry experiment need not agree with the binding enthalpy ΔH_{vH}.[15,41,43−45] Explanations for this finding are based on the fact that ΔH_{ITC} may also contain contributions of linked equilibria such as ionization or conformational changes of the protein or ligand. The next section will discuss the measured enthalpy in more detail.

DOI: 10.1021/acsomega.8b01493
ACS Omega 2018, 3, 9086−9095

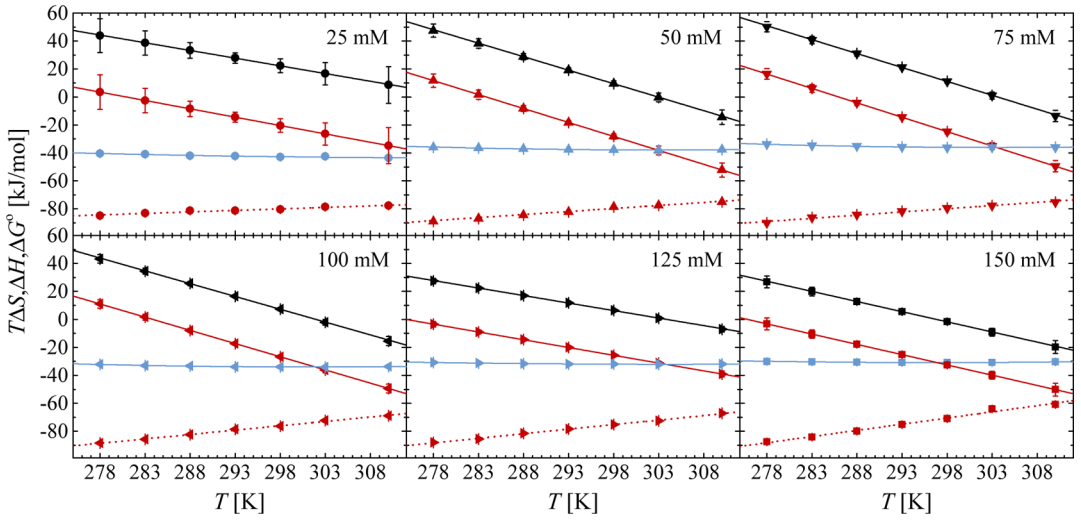

Figure 8. Entropic ($T\Delta S_{vH}$, black) and enthalpic (ΔH_{vH}, red) contributions in total free energy (ΔG^{o}, blue) at different ionic strengths. The calorimetric enthalpy ΔH_{ITC} (dashed red) is plotted as a comparison to ΔH_{vH}.

Table 2. Enthalpy Contributions of Linked Equilibria for dPGS−Lys Complexation in Phosphate Buffer at 310 K[a]

c_s [mM]	ΔH_{ITC}^{phos} [kJ/mol]	ΔH_{ITC}^{MOPS}* [kJ/mol]	Δn_{H^+}	ΔH_{ion} [kJ/mol]	ΔH_{prot} [kJ/mol]	ΔH_{prot}^{*} [kJ/mol]
25	−77.7 ± 0.5	−65.4 ± 0.4	0.62 ± 0.03	1.8 ± 0.1	−44.7 ± 12.5	−29
50	−74.9 ± 0.2	−65.2 ± 0.2	0.49 ± 0.02	1.4 ± 0.1	−24.1 ± 4.9	−23
75	−75.1 ± 0.4	−66.4 ± 0.3	0.44 ± 0.03	1.3 ± 0.1	−26.9 ± 3.7	−20
100	−69.1 ± 0.4	−64.6 ± 0.3	0.22 ± 0.02	0.6 ± 0.1	−20.3 ± 2.9	−10
125	−67.2 ± 0.6	−60.0 ± 0.2	0.36 ± 0.03	1.0 ± 0.1	−29.1 ± 1.6	−17
150	−60.9 ± 0.5	−56.7 ± 0.5	0.21 ± 0.04	0.6 ± 0.1	−11.3 ± 4.1	−10

[a] ΔH_{ITC}^{MOPS}* is taken from previous measurements.[16] According to ref 36, the ionization enthalpy $\Delta H^{o}_{ion,MOPS}$ and $\Delta H^{o}_{ion,phos}$ are 22.67 and 2.88 kJ/mol, respectively, at 310 K neglecting the salt dependence. Δn_{H^+} can then be obtained according to eq 9 and $\Delta H_{ion} = \Delta n_{H^+}\Delta H^{o}_{ion,phos}$ in phosphate buffer. ΔH_{prot} is calculated with eq 7. The protonation enthalpy ΔH^{o}_{prot} for arginine and lysine is −46 kJ/mol according to the literature.[49] Thus, the protonation enthalpy in this system can be calculated according to $\Delta H^{*}_{prot} = \Delta n_{H^+}\Delta H^{o}_{prot}$.

Binding Enthalpy Versus Calorimetric Enthalpy. The directly measured ΔH_{ITC} rises with both temperature and salt concentration (see Table 1). In general, the linear dependence of enthalpy ΔH_{ITC} on temperature corresponds to a heat capacity change $\Delta C_{p,ITC}$. Figure 8 includes the linear fitting at different salt concentrations. The exothermic process is accompanied by a positive heat capacity change (see Table 1). Notably, $\Delta C_{p,ITC}$ increases with salt concentration similar to findings made for a protein−DNA binding system.[46] The value increases with ionic strength thus suggesting an exothermic process that is repressed by ions (see the discussion of this point in ref 46). Compared to $\Delta C_{p,ITC}$, the intrinsic part $\Delta C_{p,vH}$ has opposite sign and does not depend on ionic strength within the limits of error. This is indicative of linked equilibria that compensate $\Delta C_{p,vH}$ and gives overall positive $\Delta C_{p,ITC}$.

According to Kozlov and Lohman, the observed enthalpy change by calorimetry can be split up into several contributions as[13]

$$\Delta H_{ITC} = \Delta H_{vH} + \Delta H_{prot} + \Delta H_{ion} \quad (7)$$

Thus, the calorimetric enthalpy contains the binding enthalpy ΔH_{vH}, the protonation enthalpy of free or bound protein/ligand ΔH_{prot}, and the ionization (deprotonation) enthalpy of the buffer $\Delta H_{ion} = \Delta n_{H^+}\Delta H^{o}_{ion}$ with positive Δn_{H^+} being the number of protons supplied by the buffer. ΔH^{o}_{ion} is the molar enthalpy of buffer deprotonation. Similarly, the temperature dependence gives the observed $\Delta C_{p,ITC}$ as[13]

$$\Delta C_{p,ITC} = \Delta C_{p,vH} + \Delta C_{p,prot} + \Delta C_{p,ion} \quad (8)$$

Here, $\Delta C_{p,vH}$ is due to binding. The electrostatic contribution to ΔC_p is relatively small.[47] The hydration or dehydration of nonpolar and polar solute gives large heat capacity change with different signs.[48]

Binding experiments done in two different buffer solutions with distinguishable ΔH^{o}_{ion} allow us to calculate the caloric effect of buffer ionization because the first two terms at the right side of eq 7 remain unchanged. Here, we compare the measured ΔH_{ITC} in MOPS obtained previously at 310 K and different ionic strengths[16] and phosphate buffer done here. From these data, the number of released protons at 310 K can be derived as

$$\Delta n_{H^+} = \frac{\Delta H_{ITC}^{MOPS} - \Delta H_{ITC}^{phos}}{\Delta H^{o}_{ion,MOPS} - \Delta H^{o}_{ion,phos}} \quad (9)$$

The buffer ionization enthalpies for dPGS−Lys interaction at 310 K in phosphate buffer are summarized in Table 2 taking the data obtained with the MOPS buffer as ref 16 Δn_{H^+} protons are released from the buffer and it decreases with salt concentration. The positive ionization enthalpy thus decreases with salt and is relatively small. Then, the large discrepancy between ΔH_{ITC} and ΔH_{vH} must be traced back to a negative ΔH_{prot}. The protonation enthalpy can also be estimated with Δn_{H^+} and given ΔH^{o}_{prot}; however, it depends on the species of amino acid.[49] Here, we roughly estimate the protonation enthalpy with ΔH^{o}_{prot} of lysine and arginine from

DOI: 10.1021/acsomega.8b01493
ACS Omega 2018, 3, 9086−9095

the literature.[49] The values in Table 2 are in a comparable range with the calculation according to eq 7, which indicates that positive residues at the binding site may be protonated and the protonation brings a large negative contribution to the measured enthalpy.

It should be kept in mind that the binding of several lysozyme molecules to a single dPGS is accompanied by a notable negative cooperativity. This could be seen directly in Figure 6. ΔG° refers to the situation where $\theta = \theta^*$, that is, at the inflection point of the ITC titration curve and so does ΔH_{vH} derived from eq 7. The measured enthalpy ΔH_{ITC}, on the other hand, is fitted by the starting points of an ITC isotherm at low θ. ΔH_{ITC} may differ at higher θ in cases where negative cooperativity comes into play. Hence, eq 7 and the estimates given in Table 2 can only work on a qualitative level.

CONCLUSIONS

We present a systematic thermodynamic study on complexation of dPGS-G2 with lysozyme. In particular, we measured the dependence of the binding constant on temperature and ionic strength. The dependence on salt concentration clearly revealed counterion-release as the driving force while the dependence on temperature demonstrated strong enthalpy−entropy compensation. Together with the simulations on the dPGS−lysozyme binding, the present thermodynamic analysis shows that the enthalpic and the entropic contributions compensate each other over the entire range of temperature to give a nearly constant free energy driven solely by electrostatic factors. Hence, in case of the present hydrophilic dendritic system, the driving force, namely counterion-release with electrostatic attraction, is responsible for binding while all contributions due to hydration cancel out in good approximation.

EXPERIMENTAL SECTION

Materials. The protein lysozyme from chicken egg-white with molecular weight 14.3 kDa was purchased from Alfa Aesar (J60701) and used directly. dPGS of second generation (dPGS-G2) was synthesized according to the literature.[25,50] The properties of dPGS-G2 are collected in Table 3. More details are given in our previous work.[16,24]

Table 3. Chemical Properties of dPGS[24a]

label	$M_{n,dPGS}$ [kD]	PDI	DS [%]	N_{ter}
dPGS	4.9	1.7	≥98	28

[a] $M_{n,dPGS}$: number-averaged molecular weight of dPGS; PDI: polydispersity index; DS: degree of sulfation of the terminal groups; and N_{ter}: total number of terminal sulfate groups.

Isothermal Titration Calorimetry. Sodium phosphate dibasic (10 mM; Na_2HPO_4) and 1.8 mM potassium phosphate monobasic (KH_2PO_4) were dissolved into solution, and the pH was adjusted to 7.4 at RT by adding 1 M NaOH. To prepare buffers with different ionic strengths, additional NaCl was added into the buffer individually.

ITC was used to evaluate the thermodynamics of dPGS−protein binding. The measurements were performed by a MicroCal VP-ITC instrument (GE Healthcare, Freiburg, Germany) with a syringe volume of 280 μL and a cell volume of 1.43 mL. The interaction was measured at six ionic strengths each with seven temperatures. A solution of lysozyme was located in the syringe and titrated stepwise into the cell filled with dPGS solution. The dilution heat was obtained by titrating a lysozyme solution of the same concentration into pure buffer. Figure 2 displays typical examples of experimental ITC curves. At higher salt concentration, the binding affinity became smaller and the sample concentration had to be increased to obtain a sigmoidal isotherm.[37,51] Our previous analysis showed that an increase of the sample concentration did not change the resulting binding constant (see Table S1 of ref 16). Table 4 gathers the sample concentrations used for the respective concentration of salt.

Table 4. Protein Concentration c_{Lys} and dPGS Concentration c_{dPGS} in ITC Measurements at Different Ionic Strength c_s[a]

c_s [mM]	25	50	75	100	125	150
c_{Lys} [mM]	0.11	0.24	0.56	0.87	1.31	1.36
c_{dPGS} [μM]	2.4	10.3	22.5	35.1	57.8	69.9

[a] The sample concentrations are the same for different temperatures at one ionic strength.

The raw data were analyzed with the Origin 7.0 (MicroCal) software, and the SSIS model was used to fit the isotherm.[37] The SSIS model assumes that all the binding sites are equivalent and independent. The thermodynamic data here are compared with previous ITC measurements at 310 K in a different buffer (MOPS).[16]

Molecular Dynamics Simulation. CG simulations with implicit water and explicit salt were performed as described in our previous work.[16,29] The simulation used the stochastic dynamics integrator in GROMACS 4.5.4 software package.[52] The CG model of dPGS-G2 dendrimer was established by us before and used directly here.[24] The CG model of Lysozyme (PDB: 2LZT) was constructed taking each amino acid residue as a single CG bead maintained by a structure-based Go-model force field.[53] At physiological pH, dPGS-G2 and lysozyme had net charge of −24 e and +8 e, respectively.[16] The binding between lysozyme and dPGS-G2 was conducted at 293 and 310 K each with two salt concentrations of 25 mM and 150 mM. The PMF was obtained using steered Langevin dynamics[52] with steering velocity v_p= 0.2 nm/ns and harmonic force constant K = 2500 kJ mol^{-1} nm^{-2}. All parameters were the same as in our previous work.[16]

ASSOCIATED CONTENT

Supporting Information

The Supporting Information is available free of charge on the ACS Publications website at DOI: 10.1021/acsomega.8b01493.

Analysis of counterion-release and determination of θ^* (PDF)

AUTHOR INFORMATION

Corresponding Authors

*E-mail: haag@chemie.fu-berlin.de (R.H.).
*E-mail: matthias.ballauff@helmholtz-berlin.de (M.B.).

ORCID

Qidi Ran: 0000-0002-4764-2073
Joachim Dzubiella: 0000-0001-6751-1487
Rainer Haag: 0000-0003-3840-162X

Notes

The authors declare no competing financial interest.

DOI: 10.1021/acsomega.8b01493
ACS Omega 2018, 3, 9086−9095

■ ACKNOWLEDGMENTS

The author X.X. was funded by the China Scholarship Council. The Helmholtz Virtual Institute for Multifunctional Biomaterials for Medicine and the International Research Training Group IRTG 124 funded by the German Science Foundation are gratefully acknowledged for financial support.

■ REFERENCES

(1) Miura, N.; Dubin, P. L.; Moorefield, C. N.; Newkome, G. R. Complex Formation by Electrostatic Interaction between Carboxyl-Terminated Dendrimers and Oppositely Charged Polyelectrolytes. *Langmuir* **1999**, *15*, 4245−4250.

(2) Cooper, C. L.; Dubin, P. L.; Kayitmazer, A. B.; Turksen, S. Polyelectrolyte-protein complexes. *Curr. Opin. Colloid Interface Sci.* **2005**, *10*, 52−78.

(3) Kayitmazer, A. B.; Seeman, D.; Minsky, B. B.; Dubin, P. L.; Xu, Y. Protein-polyelectrolyte interactions. *Soft Matter* **2013**, *9*, 2553−2583.

(4) Wei, Q.; Becherer, T.; Angioletti-Uberti, S.; Dzubiella, J.; Wischke, C.; Neffe, A. T.; Lendlein, A.; Ballauff, M.; Haag, R. Protein interactions with polymer coatings and biomaterials. *Angew. Chem., Int. Ed.* **2014**, *53*, 8004−8031.

(5) Xiong, W.; Ren, C.; Tian, M.; Yang, X.; Li, J.; Li, B. Complex coacervation of ovalbumin-carboxymethylcellulose assessed by isothermal titration calorimeter and rheology: Effect of ionic strength and charge density of polysaccharide. *Food Hydrocolloids* **2017**, *73*, 41−50.

(6) Record, M. T.; Anderson, C. F.; Lohman, T. M. Thermodynamic analysis of ion effects on the binding and conformational equilibria of proteins and nucleic acids: the roles of ion association or release, screening, and ion effects on water activity. *Q. Rev. Biophys.* **1978**, *11*, 103−178.

(7) Velazquez-Campoy, A.; Freire, E. Isothermal titration calorimetry to determine association constants for high-affinity ligands. *Nat. Protoc.* **2006**, *1*, 186−191.

(8) Lindman, S.; Lynch, I.; Thulin, E.; Nilsson, H.; Dawson, K. A.; Linse, S. Systematic Investigation of the Thermodynamics of HSA Adsorption toN-iso-Propylacrylamide/N-tert-Butylacrylamide Copolymer Nanoparticles. Effects of Particle Size and Hydrophobicity. *Nano Lett.* **2007**, *7*, 914−920.

(9) Kayitmazer, A. B. Thermodynamics of complex coacervation. *Adv. Colloid Interface Sci.* **2017**, *239*, 169−177.

(10) Niedzwiecka, A.; Stepinski, J.; Darzynkiewicz, E.; Sonenberg, N.; Stolarski, R. Positive Heat Capacity Change upon Specific Binding of Translation Initiation Factor eIF4E to mRNA 5' Cap. *Biochemistry* **2002**, *41*, 12140−12148.

(11) Datta, K.; LiCata, V. J. Thermodynamics of the binding of Thermus aquaticus DNA polymerase to primed-template DNA. *Nucleic Acids Res.* **2003**, *31*, 5590−5597.

(12) Datta, K.; Wowor, A. J.; Richard, A. J.; LiCata, V. J. Temperature dependence and thermodynamics of Klenow polymerase binding to primed-template DNA. *Biophys. J.* **2006**, *90*, 1739−1751.

(13) Kozlov, A. G.; Lohman, T. M. Large contributions of coupled protonation equilibria to the observed enthalpy and heat capacity changes for ssDNA binding toEscherichia coli SSB protein. *Proteins* **2000**, *41*, 8−22.

(14) Welsch, N.; Becker, A. L.; Dzubiella, J.; Ballauff, M. Core-shell microgels as smart carriers for enzymes. *Soft Matter* **2012**, *8*, 1428−1436.

(15) Geschwindner, S.; Ulander, J.; Johansson, P. Ligand binding thermodynamics in drug discovery: still a hot tip? *J. Med. Chem.* **2015**, *58*, 6321−6335.

(16) Xu, X.; Ran, Q.; Dey, P.; Nikam, R.; Haag, R.; Ballauff, M.; Dzubiella, J. Counterion-release entropy governs the inhibition of serum proteins by polyelectrolyte drugs. *Biomacromolecules* **2018**, *19*, 409−416.

(17) Dernedde, J.; Rausch, A.; Weinhart, M.; Enders, S.; Tauber, R.; Licha, K.; Schirner, M.; Zugel, U.; von Bonin, A.; Haag, R. Dendritic polyglycerol sulfates as multivalent inhibitors of inflammation. *Proc. Natl. Acad. Sci. U.S.A.* **2010**, *107*, 19679−19684.

(18) Khandare, J.; Mohr, A.; Calderón, M.; Welker, P.; Licha, K.; Haag, R. Structure-biocompatibility relationship of dendritic polyglycerol derivatives. *Biomaterials* **2010**, *31*, 4268−4277.

(19) Weinhart, M.; Gröger, D.; Enders, S.; Riese, S. B.; Dernedde, J.; Kainthan, R. K.; Brooks, D. E.; Haag, R. The Role of Dimension in Multivalent Binding Events: Structure-Activity Relationship of Dendritic Polyglycerol Sulfate Binding to L-Selectin in Correlation with Size and Surface Charge Density. *Macromol. Biosci.* **2011**, *11*, 1088−1098.

(20) Schneider, T.; Welker, P.; Licha, K.; Haag, R.; Schulze-Tanzil, G. Influence of dendritic polyglycerol sulfates on knee osteoarthritis: an experimental study in the rat osteoarthritis model. *BMC Musculoskeletal Disord.* **2015**, *16*, 387.

(21) Boreham, A.; Pikkemaat, J.; Volz, P.; Brodwolf, R.; Kuehne, C.; Licha, K.; Haag, R.; Dernedde, J.; Alexiev, U. Detecting and quantifying biomolecular interactions of a dendritic polyglycerol sulfate nanoparticle using fluorescence lifetime measurements. *Molecules* **2015**, *21*, 22.

(22) Maysinger, D.; Gröger, D.; Lake, A.; Licha, K.; Weinhart, M.; Chang, P. K.-Y.; Mulvey, R.; Haag, R.; McKinney, R. A. Dendritic polyglycerol sulfate inhibits microglial activation and reduces hippocampal CA1 dendritic spine morphology deficits. *Biomacromolecules* **2015**, *16*, 3073−3082.

(23) Sousa-Herves, A.; Würfel, P.; Wegner, N.; Khandare, J.; Licha, K.; Haag, R.; Welker, P.; Calderón, M. Dendritic polyglycerol sulfate as a novel platform for paclitaxel delivery: pitfalls of ester linkage. *Nanoscale* **2015**, *7*, 3923−3932.

(24) Xu, X.; Ran, Q.; Haag, R.; Ballauff, M.; Dzubiella, J. Charged dendrimers revisited: Effective charge and surface potential of dendritic polyglycerol sulfate. *Macromolecules* **2017**, *50*, 4759−4769.

(25) Haag, R.; Sunder, A.; Stumbé, J.-F. An approach to glycerol dendrimers and pseudo-dendritic polyglycerols. *J. Am. Chem. Soc.* **2000**, *122*, 2954−2955.

(26) Ramanadham, M.; Sieker, L. C.; Jensen, L. H. Refinement of triclinic lysozyme: II. The method of stereochemically restrained least squares. *Acta Crystallogr., Sect. B: Struct. Sci.* **1990**, *46*, 63−69.

(27) Visakh, P. M.; Bayraktar, O.; Picó, G. A. *Polyelectrolytes: Thermodynamics and Rheology*; Springer, 2014; pp 19−86.

(28) Record, M. T.; Lohman, T. M.; de Haseth, P. Ion effects on ligand-nucleic acid interactions. *J. Mol. Biol.* **1976**, *107*, 145−158.

(29) Yu, S.; Xu, X.; Yigit, C.; van der Giet, M.; Zidek, W.; Jankowski, J.; Dzubiella, J.; Ballauff, M. Interaction of human serum albumin with short polyelectrolytes: a study by calorimetry and computer simulations. *Soft Matter* **2015**, *11*, 4630−4639.

(30) Ran, Q.; Xu, X.; Dey, P.; Yu, S.; Lu, Y.; Dzubiella, J.; Haag, R.; Ballauff, M. Interaction of human serum albumin with dendritic polyglycerol sulfate: Rationalizing the thermodynamics of binding. *J. Chem. Phys.* **2018**, *149*, 163324.

(31) Lumry, R.; Rajender, S. Enthalpy-entropy compensation phenomena in water solutions of proteins and small molecules: A ubiquitous properly of water. *Biopolymers* **1970**, *9*, 1125−1227.

(32) Eftink, M. R.; Anusiem, A. C.; Biltonen, R. L. Enthalpy-entropy compensation and heat capacity changes for protein-ligand interactions: general thermodynamic models and data for the binding of nucleotides to ribonuclease A. *Biochemistry* **1983**, *22*, 3884−3896.

(33) Cooper, A.; Johnson, C. M.; Lakey, J. H.; Nöllmann, M. Heat does not come in different colours: entropy-enthalpy compensation, free energy windows, quantum confinement, pressure perturbation calorimetry, solvation and the multiple causes of heat capacity effects in biomolecular interactions. *Biophys. Chem.* **2001**, *93*, 215−230.

(34) Sedlmeier, F.; Horinek, D.; Netz, R. R. Entropy and enthalpy convergence of hydrophobic solvation beyond the hard-sphere limit. *J. Chem. Phys.* **2011**, *134*, 055105.

DOI: 10.1021/acsomega.8b01493
ACS Omega 2018, 3, 9086−9095

(35) Chodera, J. D.; Mobley, D. L. Entropy-enthalpy compensation: role and ramifications in biomolecular ligand recognition and design. *Annu. Rev. Biophys.* **2013**, *42*, 121−142.
(36) Fukada, H.; Takahashi, K. Enthalpy and heat capacity changes for the proton dissociation of various buffer components in 0.1 M potassium chloride. *Proteins* **1998**, *33*, 159−166.
(37) MicroCal. *ITC Data Analysis in Origin: Tutorial Guide*, 2004.
(38) Decher, G. Fuzzy Nanoassemblies: Toward Layered Polymeric Multicomposites. *Science* **1997**, *277*, 1232−1237.
(39) Decher, G.; Schlenoff, J. B. *Multilayer Thin Films: Sequential Assembly of Nanocomposite Materials, Second Edition*; Wiley, 2012.
(40) Henzler, K.; Haupt, B.; Lauterbach, K.; Wittemann, A.; Borisov, O.; Ballauff, M. Adsorption of β-Lactoglobulin on Spherical Polyelectrolyte Brushes: Direct Proof of Counterion Release by Isothermal Titration Calorimetry. *J. Am. Chem. Soc.* **2010**, *132*, 3159−3163.
(41) Horn, J. R.; Russell, D.; Lewis, E. A.; Murphy, K. P. van't Hoff and Calorimetric Enthalpies from Isothermal Titration Calorimetry: Are There Significant Discrepancies? *Biochemistry* **2001**, *40*, 1774−1778.
(42) Klebe, G. Applying thermodynamic profiling in lead finding and optimization. *Nat. Rev. Drug Discovery* **2015**, *14*, 95−110.
(43) Naghibi, H.; Tamura, A.; Sturtevant, J. M. Significant discrepancies between van't Hoff and calorimetric enthalpies. *Proc. Natl. Acad. Sci. U.S.A.* **1995**, *92*, 5597−5599.
(44) Haidacher, D.; Vailaya, A.; Horvath, C. Temperature effects in hydrophobic interaction chromatography. *Proc. Natl. Acad. Sci. U.S.A.* **1996**, *93*, 2290−2295.
(45) Becker, A. L.; Welsch, N.; Schneider, C.; Ballauff, M. Adsorption of RNase A on cationic polyelectrolyte brushes: a study by isothermal titration calorimetry. *Biomacromolecules* **2011**, *12*, 3936−3944.
(46) Kozlov, A. G.; Lohman, T. M. Calorimetric studies of E. coli SSB protein-single-stranded DNA interactions. Effects of monovalent salts on binding enthalpy 1 1Edited by D. Draper. *J. Mol. Biol.* **1998**, *278*, 999−1014.
(47) Gallagher, K.; Sharp, K. Electrostatic contributions to heat capacity changes of DNA-ligand binding. *Biophys. J.* **1998**, *75*, 769−776.
(48) Loladze, V. V.; Ermolenko, D. N.; Makhatadze, G. I. Heat capacity changes upon burial of polar and nonpolar groups in proteins. *Protein Sci.* **2008**, *10*, 1343−1352.
(49) Marini, M. A.; Berger, R. L.; Lam, D. P.; Martin, C. J. Thermal titrimetric evaluation of the heats of ionization of the commonly occurring amino acids and their derivatives. *Anal. Biochem.* **1971**, *43*, 188−198.
(50) Türk, H.; Haag, R.; Alban, S. Dendritic polyglycerol sulfates as new heparin analogues and potent inhibitors of the complement system. *Bioconjugate Chem.* **2004**, *15*, 162−167.
(51) Wiseman, T.; Williston, S.; Brandts, J. F.; Lin, L.-N. Rapid measurement of binding constants and heats of binding using a new titration calorimeter. *Anal. Biochem.* **1989**, *179*, 131−137.
(52) Hess, B.; Kutzner, C.; van der Spoel, D.; Lindahl, E. GROMACS 4: algorithms for highly efficient, load-balanced, and scalable molecular simulation. *J. Chem. Theory Comput.* **2008**, *4*, 435−447.
(53) Noel, J. K.; Whitford, P. C.; Sanbonmatsu, K. Y.; Onuchic, J. N. SMOG@ctbp: simplified deployment of structure-based models in GROMACS. *Nucleic Acids Res.* **2010**, *38*, W657−W661.

DOI: 10.1021/acsomega.8b01493
ACS Omega 2018, 3, 9086−9095